

# Supporting Information

## Chemiresistive electronic nose toward detection of biomarkers in exhaled breath

*Hi Gyu Moon,<sup>†,‡,⊥</sup> Youngmo Jung,<sup>‡,⊥,||</sup> Soo Deok Han,<sup>†,§</sup> Young-Seok Shim,<sup>†</sup> Beomju Shin,<sup>⊥</sup> Taikjin Lee,<sup>⊥</sup> Jin-Sang Kim,<sup>†</sup> Seok Lee,<sup>⊥</sup> Seong Chan Jun,<sup>||</sup> Hyung-Ho Park,<sup>\*,‡</sup> Chulki Kim<sup>\*,⊥</sup> and Chong-Yun Kang<sup>\*,†,§</sup>*

<sup>†</sup> Center for Electronic Materials, Korea Institute of Science and Technology (KIST), Seoul 136-791, Republic of Korea.

<sup>‡</sup> Department of Material Science and Engineering, Yonsei University, Seoul 120-749, Republic of Korea.

<sup>§</sup> KU-KIST Graduate School of Converging Science and Technology, Korea University, Seoul 136-701, Republic of Korea.

<sup>⊥</sup> Sensor System Research Center, Korea Institute of Science and Technology (KIST), Seoul 136-791, Korea.

<sup>||</sup> Department of Mechanical Engineering, Yonsei University, Seoul 120-749, Republic of Korea.

\*E-mail: chulki.kim@kist.re.kr; hhpark@yonsei.ac.kr ; cykang@kist.re.kr

## **Contents**

**Table S1.** Detection limits of H<sub>2</sub>S, NH<sub>3</sub>, and NO in 80% of RH.

**Figure S1.** 4-inch wafer (SiO<sub>2</sub> (1 μm)/Si (500 μm)) substrate with 60 single sensors and photo image (inset) of 3 x 3 sensor array with sensing layers after Au wire bonding.

**Figure S2.** The sequential processes for manufacturing the CEN by using e-beam evaporation with a GAD mode.

**Figure S3.** (A) Micro-back-heater for gas sensing measurement. (B) Integrated gateway with the CEN and conventional gas sensor.

**Figure S4.** Real-time response of each channel in the CEN to 10 ppm CO, benzene, and ethanol in 80% of RH.

**Figure S5.** Real-time response of each channel in the CEN to 4% CO<sub>2</sub> as a function of RH.

**Figure S6.** Dynamic sensing transients of the CEN to CEN to 0.2–0.8 ppm NO, 0.6–1 ppm H<sub>2</sub>S, and 1–8 ppm NH<sub>3</sub> in 80% of RH.

**Table S1.** Detection limits of H<sub>2</sub>S, NH<sub>3</sub>, and NO in 80% of RH.

		Ch1	Ch2	Ch3	Ch4	Ch5	Ch6	Ch7	Ch8	Ch9
<b>H<sub>2</sub>S</b>	rms (noise)	0.006751	0.007954	0.014396	0.020317	0.023949	0.00578	0.012372	0.012493	0.01667
	slope	12.5	27.5	15	32.5	52.5	32.5	60	17.5	50
	DL(ppb)	1.62027	0.86769	2.87912	1.87538	1.36852	0.53358	0.61862	2.14163	1.00021
<b>NH<sub>3</sub></b>	rms	0.009938	0.014099	0.015819	0.033995	0.009844	0.017502	0.019014	0.012694	0.010967
	slope	2.83784	1.0001	2.58108	2.48649	6.63514	3.06757	1.13514	2.45946	5.06757
	DL(ppb)	10.5063	42.2962	18.3865	41.0152	4.45104	17.1161	50.2512	15.484	6.49251
<b>NO</b>	rms	0.007	0.009123	0.006637	0.007191	0.010755	0.004963	0.004062	0.008005	0.007296
	slope	6.14286	45.71429	9.64286	19.28571	31.07143	15.71429	59.28571	70.71429	23.92857
	DL(ppb)	3.41874	0.59867	2.06491	1.11865	1.03845	0.94739	0.20554	0.33963	0.91471

The responses to 4% CO<sub>2</sub> show less than 0.6% in the whole range of humidity variation and they may be not to be considered in calculation of detection limit (DL). In detail, to calculate the DL, we used the DL equation from the signal processing data as below.

$$V_{x^2} = \sum (y_i - y)^2 \quad (1)$$

where  $y_i$  is the actually measured data and  $y$  is the corresponding value calculated from the polynomial fit. The rms noise is calculated as

$$rms_{noise} = \sqrt{\frac{V_{x^2}}{N}} \quad (2)$$

where  $N$  is the number of data points. The sensor noise can be calculated using the variation in the relative response change in the baseline using the root-mean-square (rms). For example, sensor noise of Au-functionalized SnO<sub>2</sub> to H<sub>2</sub>S is 0.020317.

$$DL \text{ (ppm)} = 3 \frac{rms}{slope} \quad (3)$$

By the IUPAC definition, finally, the DL can be calculated from the slope of linear curve as a function of concentration, when the real signal is 3 times the noise. Consequently, because the slope of Au-functionalized SnO<sub>2</sub> is 32.5, the H<sub>2</sub>S DL is 0.001875 ppm.

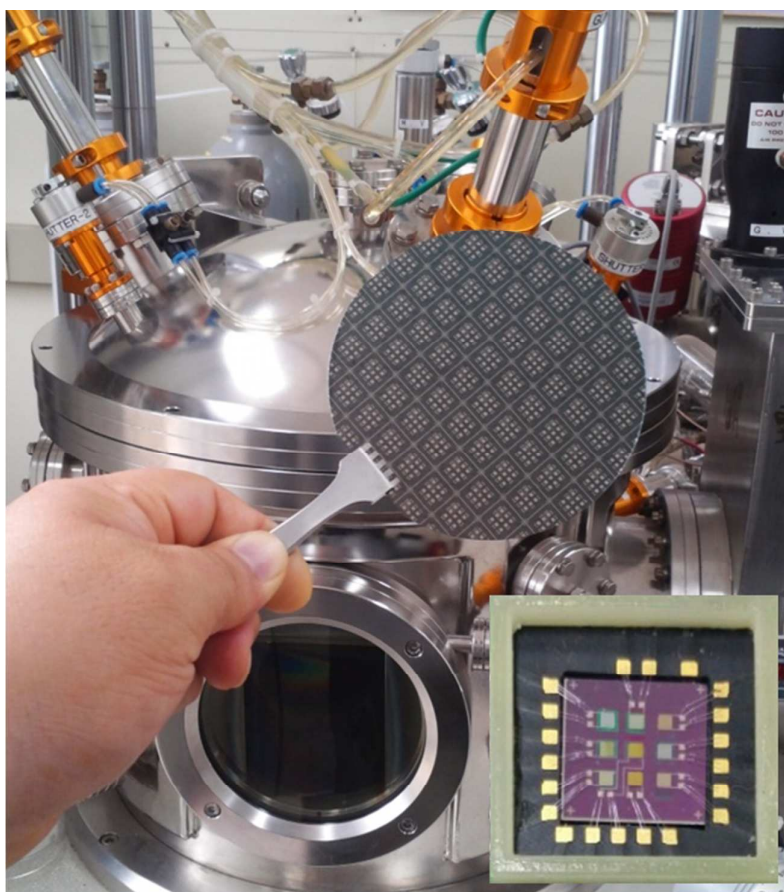


**Figure S1.** 4-inch wafer ( $\text{SiO}_2$  (1  $\mu\text{m}$ )/Si (500  $\mu\text{m}$ )) substrate with 60 single sensors and photo image (inset) of 3  $\times$  3 sensor array with sensing layers after Au wire bonding.

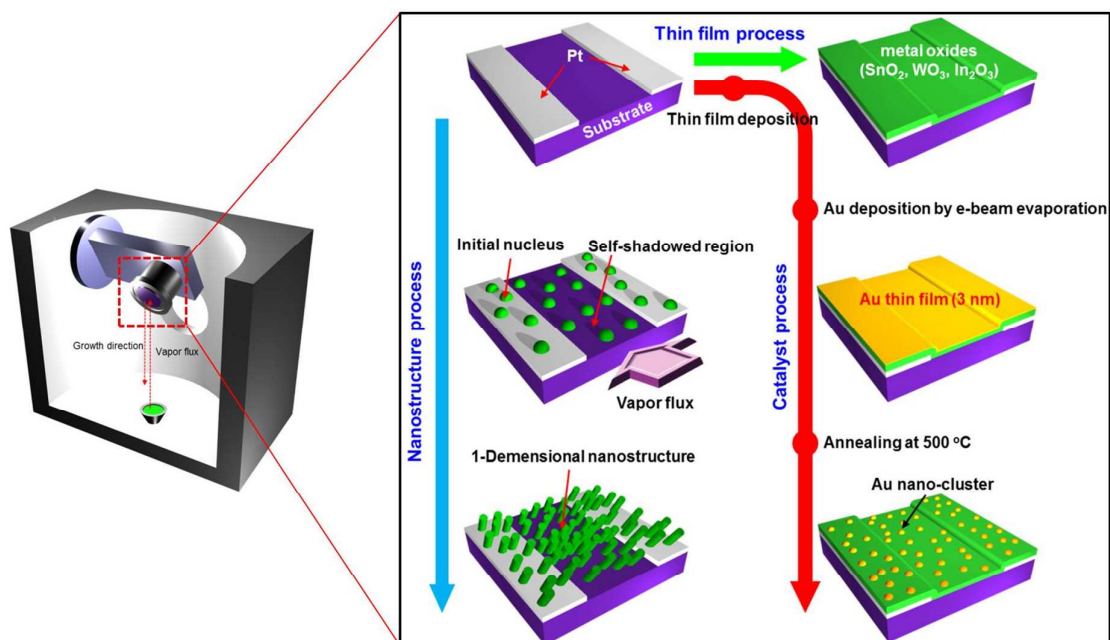


**Figure S2.** The sequential processes for manufacturing the CEN by using e-beam evaporation with a GAD mode.

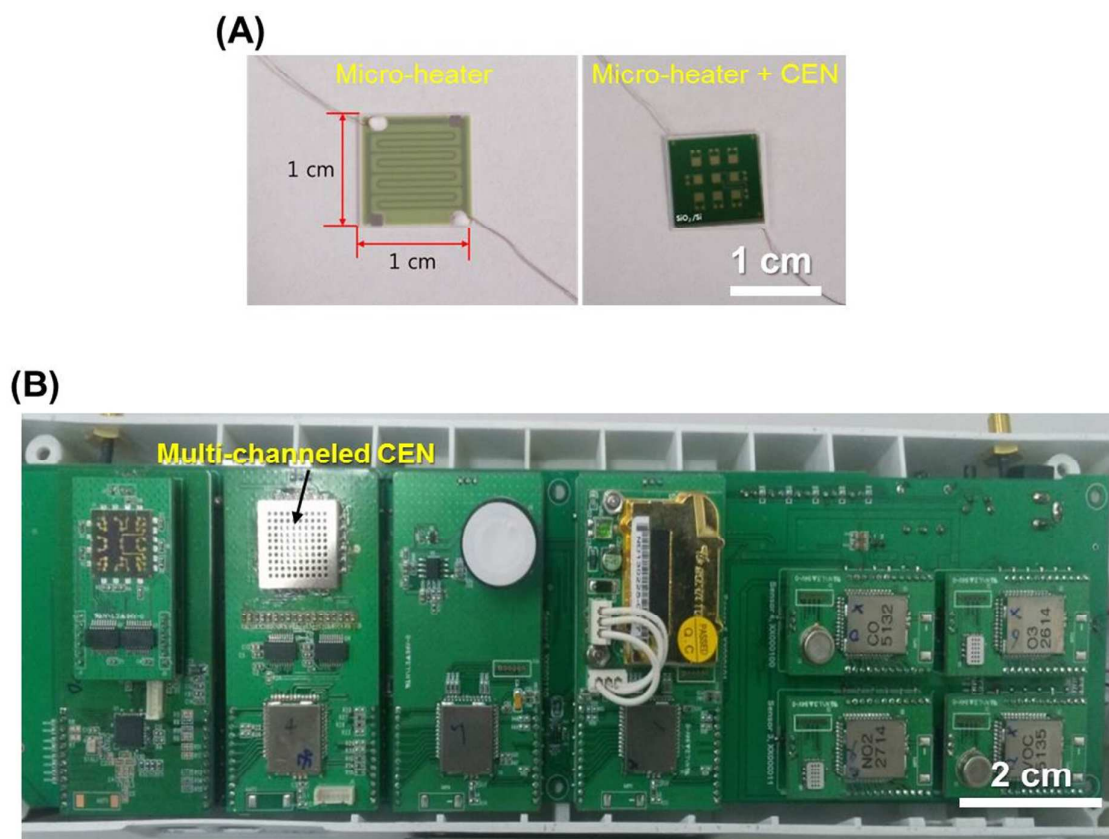


**Figure S3.** (A) Micro-back-heater for gas sensing measurement. (B) Integrated gateway with the CEN and conventional gas sensor.

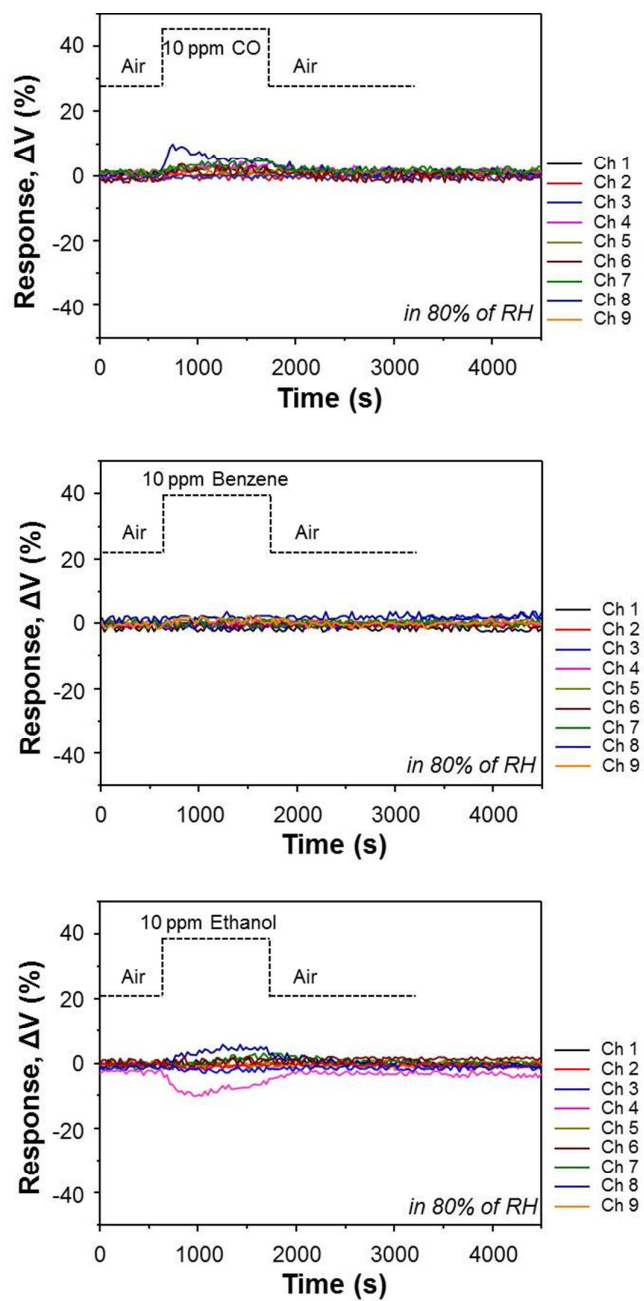


**Figure S4.** Real-time response of each channel in the CEN to 10 ppm CO, benzene, and ethanol in 80% of RH.

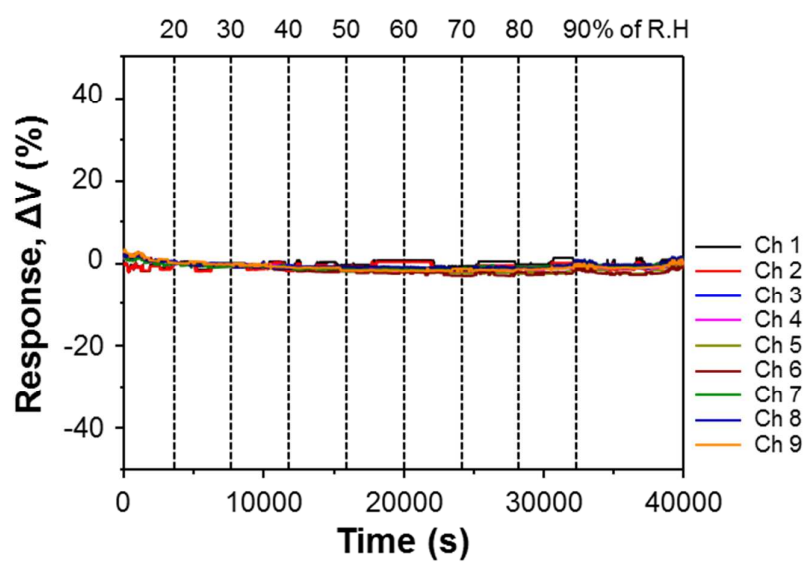


**Figure S5.** Real-time response of each channel in the CEN to 4% CO<sub>2</sub> as a function of RH.



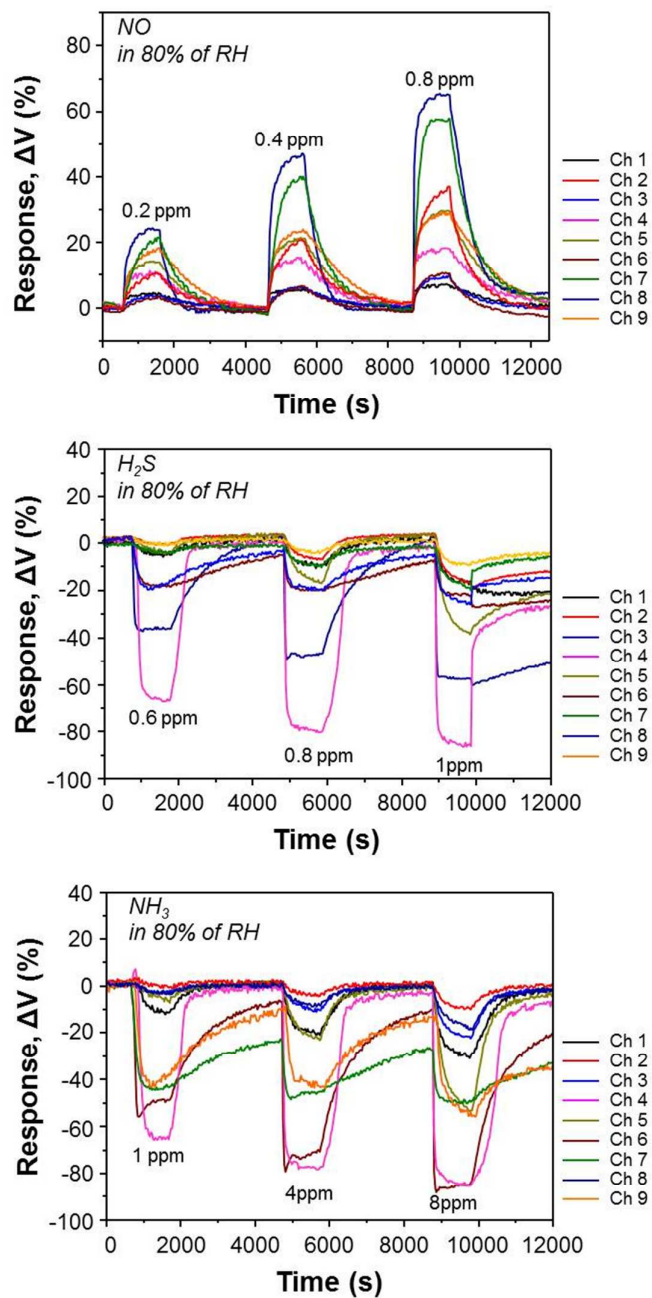


**Figure S6.** Dynamic sensing transients of the CEN to CEN to 0.2–0.8 ppm NO, 0.6–1 ppm  $H_2S$ , and 1–8 ppm  $NH_3$  in 80% of RH.